



Surface fluxes of bromoform and dibromomethane over the tropical western Pacific inferred from airborne in situ measurements

Liang Feng^{1,2}, Paul I. Palmer^{1,2}, Robyn Butler², Stephen J. Andrews³, Elliot L. Atlas⁴, Lucy J. Carpenter³, Valeria Donets⁴, Neil R. P. Harris⁵, Ross J. Salawitch⁶, Laura L. Pan⁷, Sue M. Schauffler⁷

1) National Centre for Earth Observation, University of Edinburgh, Edinburgh, UK

2) School of GeoSciences, University of Edinburgh, Edinburgh, UK

3) Department of Chemistry, Wolfson Atmospheric Chemistry Laboratories, University of York, UK

4) University of Miami, Florida, USA

5) Centre for Atmospheric Informatics and Emissions Technology, Cranfield University, Cranfield, UK

6) University of Maryland, College Park, Maryland, USA

7) National Center for Atmospheric Research, Boulder, Colorado, USA

Corresponding author: Paul I. Palmer (paul.palmer@ed.ac.uk)

ABSTRACT

We infer surface fluxes of bromoform (CHBr_3) and dibromoform (CH_2Br_2) from aircraft observations over the western Pacific using a tagged version of the GEOS-Chem global 3-D atmospheric chemistry model and a Maximum A Posteriori inverse model. The distribution of *a priori* ocean emissions of these gases are reasonably consistent with observed atmospheric mole fractions of CHBr_3 ($r=0.62$) and CH_2Br_2 ($r=0.38$). These *a priori* emissions result in a positive model bias in CHBr_3 peaking in the marine boundary layer, but capture observed values of CH_2Br_2 with no significant bias by virtue of its longer atmospheric lifetime. Using GEOS-Chem, we find that observed variations in atmospheric CHBr_3 are determined equally by sources over the western Pacific and those outside the study region, but observed variations in CH_2Br_2 are determined mainly by sources outside the western Pacific. Numerical closed-loop experiments show that the spatial and temporal distribution of boundary layer aircraft data have the potential to substantially improve current knowledge of these fluxes, with improvements related to data density. Using the aircraft data, we estimate aggregated regional fluxes of $3.6 \pm 0.3 \times 10^8$ g/month and $0.7 \pm 0.1 \times 10^8$ g/month for CHBr_3 and CH_2Br_2 over 130° – 155°E and 0° – 12°N , respectively, which represent reductions of 20–40% and substantial spatial deviations from the *a priori* inventory. We find no evidence to support a robust linear relationship between CHBr_3 and CH_2Br_2 oceanic emissions, as used by previous studies.



40 1. Introduction

The role of halogens in the catalytic destruction of stratospheric ozone is well established (WMO, 2014). The anthropogenic contribution to the inorganic halogen budget continues to decline in the stratosphere as a result of the Montreal protocol. A consequence of this
45 decline is that very short-lived substances (VSLS), halogenated compounds with e-folding lifetimes typically much less than 6 months, now represent a proportionally greater source of stratospheric halogens. The wide range of VSLS atmospheric lifetimes allow at least some of the emitted material to reach the upper troposphere, particularly over geographical regions where there is rapid, deep convection (Penkett et al., 1998; Yang et al., 2005; Warwick et al.,
50 2006; Levine et al., 2007; Pisso et al., 2010; Hosking et al., 2010; Carpenter et al., 2014; Hossaini et al., 2016a; Butler et al., 2016). Here, we use aircraft observations of bromoform (CHBr_3) and dibromomethane (CH_2Br_2) collected over the western Pacific Ocean to infer, using an inverse model, the magnitude and distribution of ocean emissions of these gases.

55 There are a wide range of VSLS that are beginning to limit the recovery of stratospheric ozone (e.g., Read et al., 2008; Hossaini et al., 2015; Oman et al., 2016). Chlorine VSLS are typically dominated by anthropogenic sources, but the fraction depends on the species (Hossaini et al., 2016b). Their natural sources include biomass burning, phytoplankton production, and soils. Iodine and bromine VSLS have predominately natural sources. Iodine
60 VSLS are mainly from ocean production processes, but with lifetimes of only a few days they are too reactive to be transported out of the marine boundary layer in large quantities. Bromine VSLS are also mainly from natural ocean sources (Gschwend et al., 1985; Manley et al., 1992; Sturges et al., 1992; Tokarczyk et al., 1994; Warwick et al., 2006; Carpenter and Liss, 2000; 2009; Palmer et al., 2009; Quack and Suess, 1999; Quack and Wallace, 2003;
65 Quack et al., 2007; Butler et al., 2007; Leedham et al., 2013). The most abundant bromine VSLS species are CHBr_3 and CH_2Br_2 . Together they account for about 80% of bromine VSLS in the marine boundary layer (Law and Sturges, 2007; O'Brien et al., 2009; Hossaini et al., 2013). The local atmospheric lifetime for CHBr_3 , determined by OH oxidation (76 days) and photolysis (36 days), is 24 days. CH_2Br_2 has a longer atmospheric lifetime of about 123
70 days, determined primarily by OH oxidation (123 days) and to a much lesser extent by photolysis (5000 days). Their lifetimes are sufficiently long that these natural halogenated compounds can be transported to the upper troposphere.



75 Previous measurement campaigns have reported that bromine VSLs and their degradation products represent 2-8 pptv of stratospheric inorganic bromine (e.g., Dorf et al., 2008; Salawich et al., 2010). Complementary model simulations of atmospheric chemistry and transport, driven by *a priori* ocean emission inventories, report similar values (2-7 pptv) that are determined mainly by localized regions of active ocean biology that coincide with strong convection. Example regions include western Pacific Ocean, tropical Indian Ocean, and off
80 the Pacific coast of Mexico. These model calculations also suggest that 15-75% of the stratospheric bromine budget from bromine VSLs is delivered by the direct transport of the emitted halogenated compounds (Liang et al., 2010; Hossaini et al., 2016a; Aschmann et al., 2009). The large range of values reflects uncertainty in ocean emissions, model transport, and the wet deposition of degradation products in the upper troposphere lower stratosphere.

85 Current knowledge of ocean emissions of CHBr_3 and CH_2Br_2 are poorly constrained by the sparse measurements. Bottom-up and top-down methods have been used to estimate global CHBr_3 and CH_2Br_2 emissions. The bottom-up approach assumes local flux estimates are representation of larger spatial scales. Ship-borne air-sea flux observations with limited
90 spatial and temporal coverage are extrapolated over ocean basins (e.g. Quack and Wallace, 2003; Carpenter and Liss, 2000; Butler et al., 2007; Ziska et al., 2013). Poor observation coverage results in fluxes that rely heavily on assumptions used for extrapolation (Stemmler et al, 2015).

95 The top-down method, in this application, uses an atmospheric chemistry transport model to describe the relationship between emissions and the atmospheric measurements. The model emissions are fitted to the observations by adjusting their magnitude until the discrepancy between the model and observed atmospheric measurements is minimized. This fitting can be achieved using heuristic techniques or more established Bayesian
100 optimization methods (e.g. Liang et al, 2010, Ordonez et al, 2012, Ashfold et al., 2014). The short atmospheric lifetime of CHBr_3 poses particular difficulties for the top-down approach because atmospheric mole fractions are highly variable (Ashfold et al, 2014). Some studies have introduced (explicitly or implicitly) a simple linear correlation between CHBr_3 and CH_2Br_2 emissions to provide an additional constraint on the CHBr_3 flux estimate (e.g. Liang
105 et al., 2010, Ordóñez et al., 2012). This approach, however, is then subject to errors associated with the assumption about the correlation. As with the bottom-up method, the top-down method is subject to errors due to poor spatial and temporal coverage of observations. By virtue of various assumptions made (and justified) by individual studies the resulting bottom-up and top-down CHBr_3 and CH_2Br_2 fluxes are significantly different (e.g.



110 Hossaini et al., 2016a). For example, the estimated global CHBr_3 annual emissions range
from 216 Tg (Ziska et al., 2013) to 530 Tg (Ordóñez et al., 2012).

We use data from two coordinated aircraft campaigns over the western Pacific during 2014
to infer regional emission estimates of CHBr_3 and CH_2Br_2 for the campaign period using a
115 Bayesian inverse model. The Co-ordinated Airborne Studies in the Tropics (CAST; Harris et
al., 2017), and CONvective Transport of Active Species in the Tropics (CONTRAST; Pan et
al., 2016) campaigns measured a suite of trace gases and aerosols centred on the
Micronesian region in the western Pacific, including Guam, Chuuk, and Palau during
January and February 2014. We interpret aircraft measurements of CHBr_3 and CH_2Br_2 mole
120 fraction using the GEOS-Chem atmospheric chemistry transport model and a Maximum A
Posteriori (MAP) inverse model approach.

In the next section we describe the CAST and CONTRAST CHBr_3 and CH_2Br_2 mole fraction
data, the GEOS-Chem atmospheric chemistry transport model used to interpret the data,
125 and the MAP inverse model. In section 3, we report a model comparison with the CAST and
CONTRAST atmospheric data, and results from the MAP inversion. We conclude the paper
in section 4.

2. Data and Methods

130

We use CHBr_3 and CH_2Br_2 mole fraction determined using GC/MS from whole air sample
(WAS) canisters collected during the CAST and CONTRAST aircraft campaigns during
January 18th to February 28th, 2014 (Harris et al., 2017; Pan et al., 2016). We refer the
reader to Andrews et al. (2016) for a more detailed description of the observation data sets,
135 and to Butler et al (2016) for a statistical analysis of the CHBr_3 and CH_2Br_2 mole fraction
data. For CAST, WAS canisters were filled aboard the Facility for Airborne Atmospheric
Measurements (FAAM) BAe-146 UK Atmospheric Research Aircraft. These canisters were
analysed for CHBr_3 and CH_2Br_2 and other trace compounds within 72 hours of collection.
The WAS instrument was calibrated using the National Oceanic and Atmospheric
140 Administration (NOAA) 2003 scale for CHBr_3 and the NOAA 2004 scale for CH_2Br_2 (Jones et
al., 2011; Andrews et al., 2016). For CONTRAST, a similar WAS system was employed to
collect CHBr_3 and CH_2Br_2 measurements on the NSF/NCAR Gulfstream-V HIAPER (High-
performance Instrumented Airborne Platform for Environmental Research) aircraft. A
working standard was used to regularly calibrate the samples, and the working standard was
145 calibrated using a series of dilutions of high concentration standards that are linked to
National Institute of Standards and Technology standards. The mean absolute percentage



error for CHBr_3 and CH_2Br_2 measurements between 0–8 km is 7.7% and 2.2% between the two WAS systems and two accompanying GC/MS instruments, respectively.

150 To interpret these atmospheric data we use the GEOS-Chem global 3-D atmospheric
chemistry transport model (v9.03, <http://geos-chem.org>). We drive the GEOS-Chem model
using GEOS-FP meteorological fields, provided by the Global Modeling and Assimilation
Office at NASA Goddard, with a horizontal resolution of 2° (latitude) X 2.5° (longitude). We
use a tagged version of the model (Butler et al, 2016) in which the atmospheric chemistry is
155 linearized by using pre-computed OH and photolysis loss terms using the same version of
the model but with a more complete description of HOx-NOx-Ox and bromine chemistry
(Parrelle et al., 2012). Our 3-D OH fields are consistent with the observed methyl chloroform
lifetime. We find small (5%) adjustments to these OH fields do not significantly affect our
analysis or conclusions (not shown). For the purpose of our calculations we pre-compute
160 these loss terms every three hours during the campaign. This tagged modelling approach
greatly simplifies the calculation of the Jacobian matrix used by the inverse model to
determine surface flux estimates, as described below. We have previously evaluated this
version of the model using CHBr_3 and CH_2Br_2 mole fraction data from NOAA/ESRL (Butler et
al, 2016), and showed a level of agreement with *in situ* observations that is comparable to
165 the ensemble of models reported by Hossaini et al (2016a).

We use *a priori* emissions of CHBr_3 and CH_2Br_2 from the Ordóñez et al (2012) inventory,
which is based on the top-down methodology using aircraft observations from 1996 to 2006.
This represents one of three commonly used inventories, which were recently evaluated in a
170 multi-model inter-comparison study (Hossaini et al, 2016a). Liang et al (2010) also employed
a top-down methodology to infer CHBr_3 and CH_2Br_2 fluxes, but Ziska et al. (2013) inferred
these fluxes from a database of surface ocean observations collected from 1989 to 2011.
We find no single inventory is best at reproducing observations of both gases. Ordóñez et al
(2012) assumed a linear relationship between tropical CHBr_3 and CH_2Br_2 emissions and
175 monthly fields of chlorophyll-a, a proxy for ocean biological activity, to help fill in the spatial
and temporal gaps left by the aircraft data. This approach strongly links the distributions of
these two gases in the *a priori* inventory, an assumption we examine below. We primarily
use Ordóñez et al. (2012) but also show the results from other inventories. For our study
period, these aggregated regional fluxes are $6.2 \pm 0.9 \times 10^8$ g/month and $0.9 \pm 0.2 \times 10^8$ g/month
180 for CHBr_3 and CH_2Br_2 over 130° – 155°E and 0° – 12°N , respectively.

Figure 1 shows the geographical regions considered in this study. We divide the world into
605 basis functions: 1) a nested domain of 600 grid-scale tagged regions over the tropical



western Pacific (105°—165°E, -15°—25°N); 2) a lateral boundary of 15° surrounding the
185 nested domain, described by four tagged regions; and 3) the rest of the world. We spin-up
the model using *a priori* inventories (Ordóñez et al., 2012) from July 1st 2013 to January 18th
2014, reducing the impact of initial conditions.

We use the MAP approach to infer CHBr₃ and CH₂Br₂ surface fluxes from atmospheric mole
190 fraction measurements taken by CAST and CONTRAST aircraft campaigns. We infer
regional monthly mean surface fluxes, f , of CHBr₃ and CH₂Br₂:

$$f_p^g(x) = f_0^g(x) + \sum_i c_i^g BF_i^g(x), \quad (1)$$

where superscript g denotes trace gas, and the subscripts 0 and p denote the *a priori* and *a*
posteriori state vector, respectively. We describe the regional fluxes as a product of a basis
195 function set $BF_i^g(x)$, representing distributions of monthly mean fluxes of the study gases
over 605 pre-defined geographic regions (Figure 1) over the duration of the CAST and
CONTRAST aircraft experiments, and scalar coefficients c_i^g that are fitted to the data.

We include all the coefficients c_i^g for the pre-defined 605 basis functions into the state vector
200 \mathbf{c} that describes the CHBr₃ and CH₂Br₂ fluxes, which we fit to the observations. We take into
account the uncertainty of the model spin-up by including a scaling factor into the state
vector to adjust the background (initial) field, assuming that the model describes the
background vertical structure over the study domain. As a result the state vector \mathbf{c} has a
total of 606 elements. We optimally estimate the state vector \mathbf{c} by minimizing the associated
205 cost function $J(\mathbf{c})$:

$$J(\mathbf{c}) = \frac{1}{2} [\mathbf{c} - \mathbf{c}_0]^T \mathbf{B}^{-1} [\mathbf{c} - \mathbf{c}_0] + \frac{1}{2} (\mathbf{y}_{obs} - H(\mathbf{c}))^T \mathbf{R}^{-1} (\mathbf{y}_{obs} - H(\mathbf{c})), \quad (2)$$

where the superscripts T and -1 denote the matrix transpose and inverse operations,
respectively; \mathbf{c}_0 represents the *a priori* estimates; and \mathbf{B} represents the *a priori* error
covariance matrix. The measurement vector, including the CAST/CONTRAST CHBr₃ and
210 CH₂Br₂ mole fraction data, is denoted by \mathbf{y}_{obs} , and \mathbf{R} is the measurement error covariance
matrix. The forward model H projects the state vector (scalar coefficients) into observation
space (3-D mole fractions), and includes the GEOS-Chem atmospheric chemistry and
transport model that is sampled at the time and location of each observation.

215 We assume a 60% uncertainty for fluxes within the nested domain and a 50% uncertainty for
fluxes in the lateral boundary and the rest of the world regions, guided by the discrepancy
between the top-down and bottom-up inventories and their limited spatial and temporal
variation. We also assume that the *a priori* errors within the nested domain are correlated
over a distance of 400 km, corresponding to approximately the width of two adjacent grid



220 boxes. We assume the initial conditions for the mole fractions have a 30% uncertainty. We
assume individual observations of CHBr_3 and CH_2Br_2 have errors of 20% and 10%,
respectively, and are uncorrelated. These conservative values are guided by an analysis of
data collected from different instruments during CAST and CONTRAST (Andrews et al,
2016). We assume that the observation error covariance \mathbf{R} is diagonal, which also includes
225 model error, such as the representation error and the errors in modelling atmospheric
transport and chemistry processes, with an assumed value of 20%.

The Jacobian matrix describes the sensitivity of atmospheric CHBr_3 and CH_2Br_2 CAST and
CONTRAST measurements to changes in geographical surface emissions and the initial
230 value on January 18th 2014. We construct it by scaling the tagged tracers originating from a
specific geographical region by surface fluxes from that region.

To avoid negative flux estimates due to, for example, an uneven distribution of observations
we use value-dependent prior uncertainties for grid point flux estimates. We assume a
235 functional form for the uncertainty of the flux coefficient c_i (equation 1):

$$\sigma(c_i) = \begin{cases} 0.8, & c_i > -0.6 \\ 0.8 - 2(-0.6 - c_i)e^{k(1.0+c_i)}, & c_i < -0.6, \end{cases} \quad (3)$$

where k ($=3$) is a pre-chosen factor that defines the gradient of the uncertainty with respect
to the change of c_i . Using this approach, the *a priori* uncertainty decreases rapidly towards
zero when c_i becomes smaller than -0.6 (i.e., when the flux estimate is smaller than 40% of
the *a priori*). We find that using different parameters (e.g. changing the threshold from -0.6 to
240 -0.8) does not significantly change our flux estimates.

3 Results

245 Forward Model Analysis

Figure 2 shows that the model overestimates the CHBr_3 concentrations by 0.1—0.7 pptv at
altitudes from 0.5 to 12.5 km, with the largest values near the surface that reflects errors in a
priori ocean fluxes (Hossaini et al., 2016a; Butler et al, 2016). The model has reasonable
skill at reproducing the mean observed vertical gradient ($r=0.62$) but has a positive model
250 bias of 0.46 ± 0.39 pptv. We find that vertical variations in CHBr_3 are determined
approximately equally by sources over the western Pacific study region (Figure 1) and by
sources immediately outside of the nested domain and further afield (Butler et al, 2016).
These contributions show different vertical structures. The contribution from fresher sources
over the western Pacific has a steeper atmospheric lapse rate from the boundary layer to the



255 free troposphere than the air masses from neighbouring regions. Both contributions are
approximately uniform above the free troposphere, with the exception of a peak at 10–12 km
from the air being transported into the nested domain (Butler et al, 2016). These differences
in vertical structure help the inversion system identify the origin of CHBr_3 at different vertical
levels.

260

The model reproduces some of the observed CH_2Br_2 variation ($r=0.38$) but with a small
mean bias (0.01 ± 0.14 pptv). Figure 2 shows that the CH_2Br_2 source outside the nested
domain represent more than 60% ($0.7\text{--}0.9$ pptv) of the values sampled over the western
Pacific, and almost invariant with altitude. This is due to weaker surface emissions over the
265 western Pacific and the longer atmospheric lifetime of CH_2Br_2 compared to CHBr_3 . Ocean
emissions from the western Pacific and from the immediate neighbouring regions each
contribute only $0.1\text{--}0.3$ pptv to CH_2Br_2 . This highlights the difficulties of inferring ocean
fluxes of CH_2Br_2 only using atmospheric CH_2Br_2 data collected over the western Pacific and
considering this region in isolation.

270

To examine model transport errors associated with using a relatively coarse model spatial
resolution ($2^\circ\times 2.5^\circ$), we ran a short, high-resolution ($0.25^\circ\times 0.3125^\circ$) simulation of CHBr_3 over
a limited spatial domain centred on the western Pacific and compared that against the
CAST/CONTRAST data. We acknowledge that we could still miss rapid, sub-grid scale
275 convective events using this model that has a factor-of-eight improvement in spatial
resolution. However, we find that differences between the two model runs are much smaller
than the differences between the individual model runs and the observations (Figure 2),
suggesting that our model bias is mostly a result of overestimating ocean sources.

280 Closed-Loop Numerical Experiments

In the absence of independent observations to evaluate our *a posteriori* ocean fluxes we use
closed-loop numerical experiments to understand what we can theoretically achieve from
CAST and CONTRAST data, accounting for a realistic description of model and
measurement errors. These calculations, often called observing system simulation
285 experiment (OSSEs), provide an upper boundary on the ability of available data to infer the
true state.

First, we generate synthetic observations at the time and location of the CAST and
CONTRAST data by sampling 3-D model fields of CHBr_3 and CH_2Br_2 mole fraction driven by
290 the *a priori* inventories, which we regard as the ‘true’ emissions. We consider these sample



mole fraction values as the instrument observation after we superimpose instrument (unbiased) noise, informed by realistic observation uncertainty. Second, we enlarge the ('true') *a priori* emissions to generate the *a priori* estimate for the OSSEs: by 50% for emissions over the western Pacific and by 30% for emissions from the neighbouring region.

295 The resulting atmospheric mole fractions represent our model *a priori* concentrations. With perfect coverage of the atmosphere with perfect data (i.e. infinitesimal noise levels) fitting model emissions to the true observations would result in estimating the true ocean emissions. We describe our results as the difference between the *a posteriori* and true fluxes using a metric (Palmer et al, 2000; Feng et al, 2009) that describes the error reduction

300 $\gamma = 1 - \sigma_a/\sigma_f$, where σ_a and σ_f denote the *a posteriori* and *a priori* uncertainties, respectively, ignoring the correlation between state vector elements. The closer the value of γ is to unity the larger reduction in uncertainty.

Figure 3 shows that the CAST/CONTRAST CH_2Br_2 and CHBr_3 measurements can

305 reproduce the true fluxes, mainly between $135\text{-}155^\circ\text{E}$ and $3^\circ\text{S}\text{-}15^\circ\text{N}$, by reducing the inflated *a priori* flux estimate. *A posteriori* fluxes in several grid boxes are lower than the true value, which is a result of regions overcompensating for other regions that have insufficient data to estimate their emissions. Regions influenced with fewer measurements (Figure 1) generally have smaller reductions in error, as expected. The error reductions for CHBr_3 range from 0.1

310 to 0.6 over the study domain, reflecting the widespread sensitivity of the CAST and CONTRAST observations to emissions from the tropical western Pacific region. The mean and median *a posteriori* fluxes are approximately a factor of three closer than the *a priori* to the true fluxes, with a 40% improvement in the uncertainties. In contrast, for CH_2Br_2 , the error reduction is much smaller, with values greater than 0.3 only over a small geographical

315 region where the data density is greatest. There is a factor-of-two improvement in the discrepancy of the fluxes with the 'true', and a 30% improvement in the uncertainties. This large improvement in the knowledge of flux estimates is partly due to our simple description of the difference between the true and *a priori* field.

320 Ocean Emissions of CHBr_3 and CH_2Br_2 Inferred from CAST/CONTRAST data

We now examine the fluxes inferred from the CAST and CONTRAST measurements. Figure 4 shows elevated *a posteriori* CHBr_3 emissions surrounding small islands north of the tropics, such as Palau (7.4°N , 134.5°E) and Chuuk ($7^\circ 25' \text{N}$, $151^\circ 47' \text{E}$). However, we find that emissions surrounding Guam (13.5°N , 144.8°E) are not significantly different from

325 the adjacent open ocean. This reflects the distribution of boundary layer measurements (altitudes $<2.5 \text{ km}$) of CHBr_3 observed during CAST and CONTRAST flights (Figure 1). We



find that through sensitivity experiments (not shown) that the *a posteriori* emissions are inferred by data and not via spatial correlations in the *a priori* emission inventory. Our *a posteriori* CHBr_3 emissions are generally higher than the bottom-up estimates from Ziska et al (2013), particularly over north of tropics.

We find that our *a posteriori* CH_2Br_2 emission estimates are lower than *a priori* estimates over open oceans north of 5°N . We also find elevated fluxes around islands and part of open oceans south of 5°N . Similar to CHBr_3 , these elevated fluxes coincide with large boundary layer measurements from CAST and CONTRAST.

Over the study domain (130° – 155°E and 0° – 12°N) our *a posteriori* fluxes are $3.6 \pm 0.3 \times 10^8$ g/month and $0.7 \pm 0.1 \times 10^8$ g/month for CHBr_3 and CH_2Br_2 , respectively. These represent reductions of 40% and 20% relative to the *a priori* values, respectively. We find that our flux estimates are largely insensitive to small changes in the assumed observation and *a priori* errors (not shown). The corresponding *a posteriori* mole fractions of CHBr_3 and CH_2Br_2 (not shown) have smaller mean biases (-0.03 ± 0.22 , -0.1 ± 0.11) and improved correlations ($r=0.74$, $r=0.56$) than the *a priori* values compared to the observations.

The spatial gradient we find in our *a posteriori* CHBr_3 emissions between the coasts of Palaua and Chuuk and the surrounding open oceans is not present in our *a priori* emission inventory (Ordóñez et al, 2012). It is, however, qualitatively consistent with observations (e.g., O'Brien et al., 2009; Quack et al., 2007) and bottom-up estimates (e.g., Ziska et al., 2013 and Simmerler et al., 2015). These elevated coastal emissions also improve the fit to CAST and CONTRAST observation particularly between 6-10 km. Figure 4 shows that the spatial distribution of *a priori* and *a posteriori* CH_2Br_2 emissions from the open ocean is different from the climatological bottom-up emissions (Ziska et al, 2013), particularly south of 5°N . This is surprising because studies have shown that tropical ocean emissions of CH_2Br_2 are correlated with the distribution of chlorophyll-a (e.g., Liu et al., 2013), but differences may reflect inter-annual changes in ocean biology.

Figure 5 shows the *a priori* and *a posteriori* CHBr_3 : CH_2Br_2 flux ratios. The top down inventory of Ordóñez et al (2012) use a linear model to describe emissions from these two gases, but the bottom-up inventory by Ziska et al, (2013) develop the emissions independently using a database of ocean observations. This discrepancy between the two inventories is why we chose not to exploit this linear relationship in our MAP inversion. Our *a posteriori* emissions for CHBr_3 and CH_2Br_2 appear to be linearly related at low emissions but larger values appear



to follow a more complicated relationship, which may reflect differences in the responsible ocean biological processes.

365

4. Summary and Concluding Remarks

Very short-lived brominated gases have predominately natural sources, and therefore cannot be regulated by international agreements (Oman et al., 2016; Butler et al., 2007).

370

Current understanding of these natural sources is poor due to the infrequent and incomplete measurements of ocean fluxes that vary in space and time. Past studies have relied on developing bottom up inventories using a database of ship-borne measurements or an heuristic top down method that adjusted *a priori* emissions to match tropospheric and lower stratospheric measurements of a range of gases, including of CHBr_3 and CH_2Br_2 . As a consequence of the uncertainties associated with the modelling and data, the resulting inventories adopt simple distributions and are not necessarily consistent with each other on regional spatial scales.

375

Here, we used an *a priori* inventory to reproduce observed atmospheric boundary layer variations of CHBr_3 and CH_2Br_2 over a small geographical region encompassing Guam, Pilau and Chuuk over the western Pacific. The measurements were collected as part of the CAST and CONTRAST aircraft campaigns during January and February 2014. We use the GEOS-Chem atmospheric chemistry model to relate the *a priori* emissions to the atmospheric concentrations, and develop a MAP inverse model to infer the ocean fluxes that correspond with the aircraft measurements.

380

385

First, using a small number of closed-loop numerical experiments we showed that the aircraft data could in theory, using assumptions about their uncertainties, improve knowledge of ocean fluxes. Improvements in knowledge are generally related to the density of measurements, as expected.

390

Using the aircraft data we find substantial spatial variations in fluxes of both gases that differ significantly from the *a priori* inventory. We find that aggregated regional *a posteriori* fluxes of CHBr_3 ($3.6 \pm 0.3 \times 10^8$ g/month) and CH_2Br_2 ($0.7 \pm 0.1 \times 10^8$ g/month) are 40% and 20% lower than the *a priori* fluxes over the study domain (130° – 155°E and 0° – 12°N). Using the model we find that observed variations of CHBr_3 are determined mainly by the open ocean while CH_2Br_2 has a large influence from outside the immediate study region. *A posteriori* fluxes significantly improve the mean observed vertical gradient of both gases, particularly in the free troposphere. We also find no evidence to suggest a robust linear relationship between

395



400 the emissions of these two gases over the study region, unlike one of the top-down *a priori*
inventories. This discrepancy may reflect differences in the analysis of data over different
spatial scales, or the construction of the *a priori* inventory using data in the free and upper
troposphere where observed air masses originating from disparate surface sources have
time to mix.

405

The MAP approach we used fits *a posteriori* fluxes to minimize the discrepancy between
model and observed atmospheric mole fractions. Any discrepancy in atmospheric data may
result from errors in surface fluxes (emissions minus uptake), atmospheric chemistry, and
atmospheric transport. The next most likely source of error is atmospheric transport,
410 particularly sub-grid scale vertical mixing. Sensitivity tests that crudely account for model
errors suggest that the *a posteriori* fluxes are robust.

Our paper highlights the value of using atmospheric data to improve the magnitude and
distribution of ocean emissions of halogenated gases, but also shows some of the difficulties
415 associated with interpreting these data even with the aid of an atmospheric transport model.
Future scientific progress in quantitatively understanding the role of natural emissions of
halogens in the catalytic destruction of stratospheric ozone is hampered by the lack of
available observations.

420 **Author contributions.**

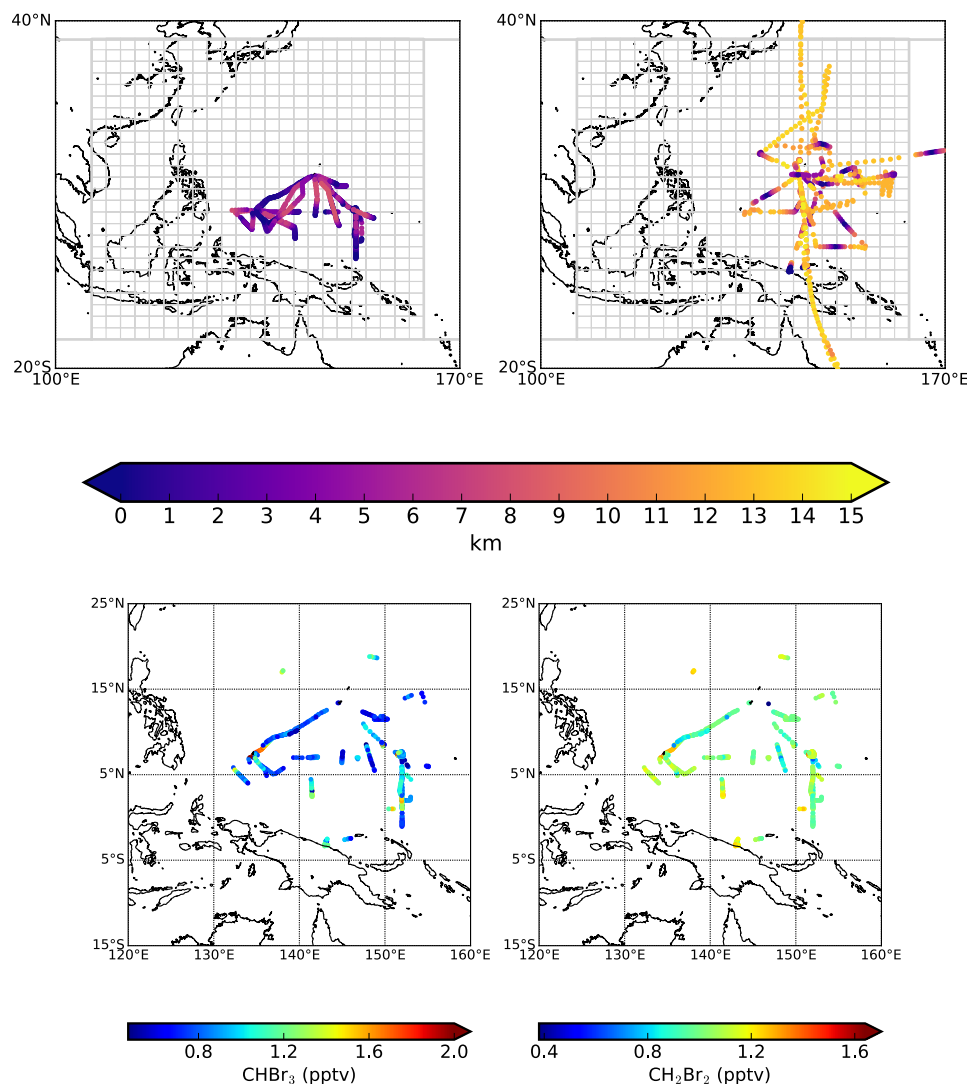
L.F, P.I.P and R.B designed the computational experiments; P.I.P. and L.F. wrote the paper;
all authors provided input on data analysis shown in the paper; the CAST and CONTRAST
team provided access to CHBr_3 and CH_2Br_2 data.

425 **Acknowledgements**

L.F. was funded by United Kingdom Natural Environmental Research Council (NERC) grant
NE/J006203/1, R.B. was funded by NERC studentship NE/1528818/1, and P.I.P. gratefully
acknowledges his Royal Society Wolfson Research Merit Award. CAST is funded by NERC
and STFC, with grants NE/ I030054/1 (lead award), NE/J006262/1, 472 NE/J006238/1,
430 NE/J006181/1, NE/J006211/1, NE/J006061/1, NE/J006157/1, NE/J006203/1, NE/J00619X/1
(University of York CAST measurements), and NE/J006173/1. We are grateful to the
Harvard University GEOS-Chem group who maintains the model. E.A. acknowledges
support from NSF Grant AGS1261689 and thanks R. Lueb, R. Hendershot, X. Zhu, M.
Navarro, and L. Pope for technical and engineering support. The CONTRAST experiment is
435 sponsored by the NSF. CONTRAST data are publicly available for all researchers and can
be obtained at http://data.eol.ucar.edu/master_list/?project=CONTRAST. The NOAA surface
data is available at <http://www.esrl.noaa.gov/gmd/dv/ftpdata.html>.



Figures



440

Figure 1 Distributions of data from the (left) CAST and (right) CONTRAST aircraft campaigns during January and February 2014. Data are described on 2° (latitude) \times 2.5° (longitude) GEOS-Chem grid boxes. The top panels show the altitude of data collected by both campaigns. We superimpose the flux inversion domain (grey lattice), consisting of 600 grid boxes between 105° – 165° E and -15° – 25° N, four larger neighbouring regions, and the rest of world. The bottom panels show the distributions of boundary layer (less than 2.5 km) CHBr_3 (pptv) and CH_2Br_2 (pptv) mole fraction data.

445



450

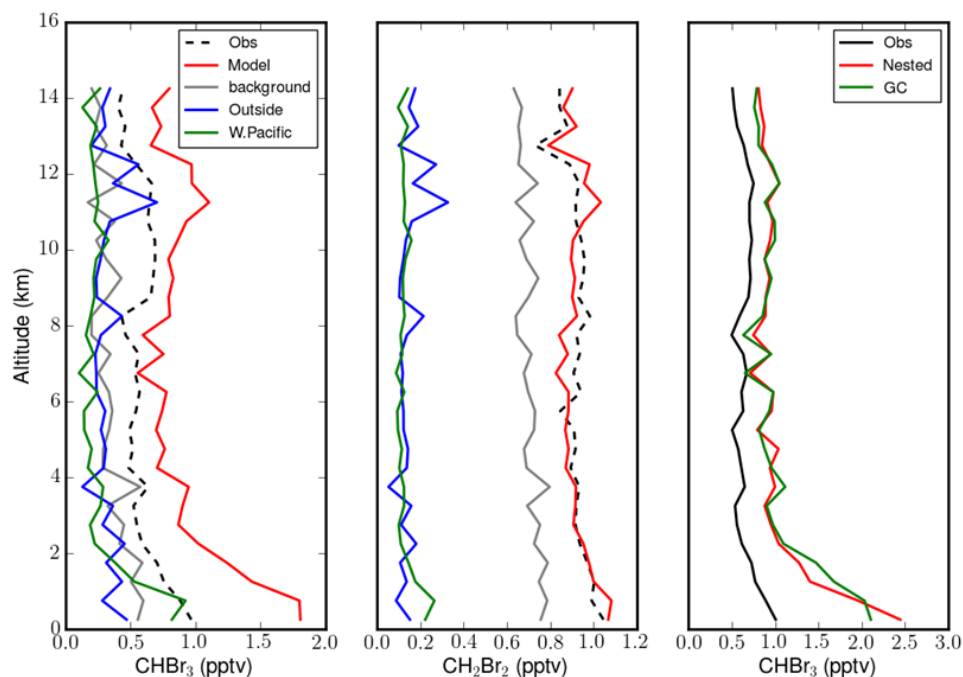


Figure 2: Observed and model mean vertical profiles of (left) CHBr_3 (pptv) and (middle) CH_2Br_2 (pptv) from the CAST and CONTRAST campaigns, described on a 1 km resolution grid. Model values have been sampled at the time and location of each observation. Also shown are the model contributions to these gases from within the Western Pacific study region, immediately outside the study region, and further afield which we denote as background values. The right panel compares CAST/CONTRAST observations of CHBr_3 with GEOS-Chem model simulations using the standard ($2.0^\circ \times 2.5^\circ$) and nested ($0.25^\circ \times 0.3125^\circ$) spatial resolutions from January 18th to February 13th, 2014. Both model runs use common emission inventories.

465



470

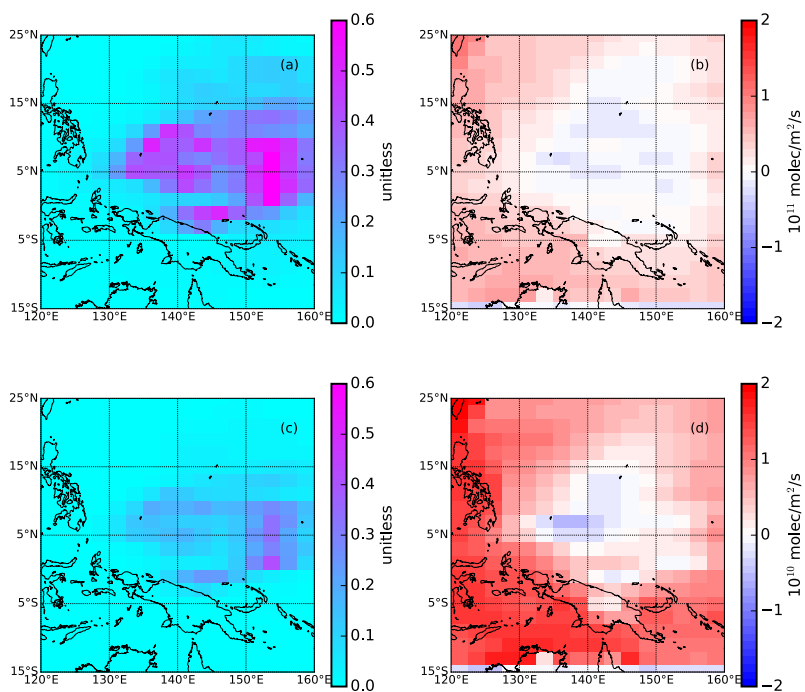


Figure 3: Simulated error reductions (unitless) and *a posteriori* flux error distributions (10^{10} molec/m²/s) of (top) CHBr₃ and (bottom) CH₂Br₂ based on the theoretical potential to recover true fluxes using the time and location of CAST and CONTRAST data.

475

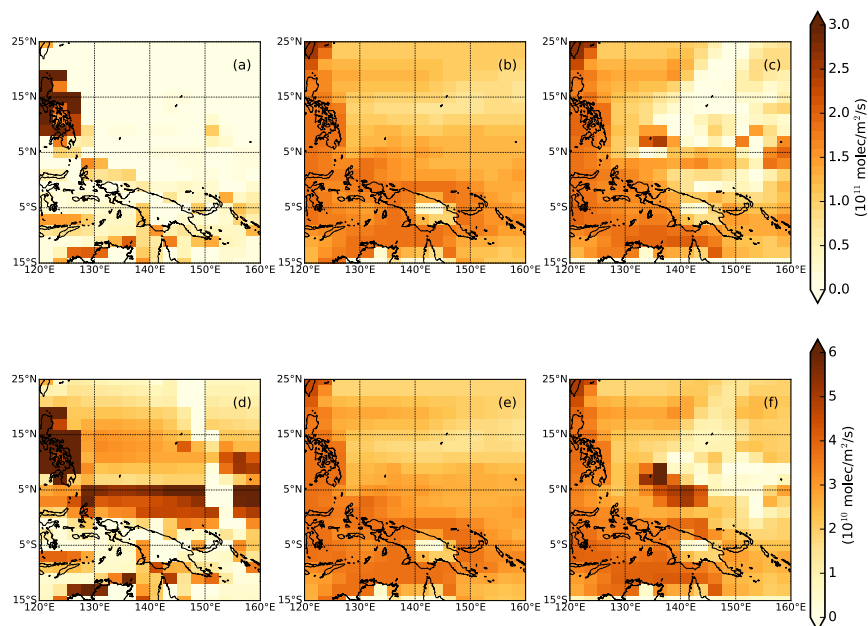
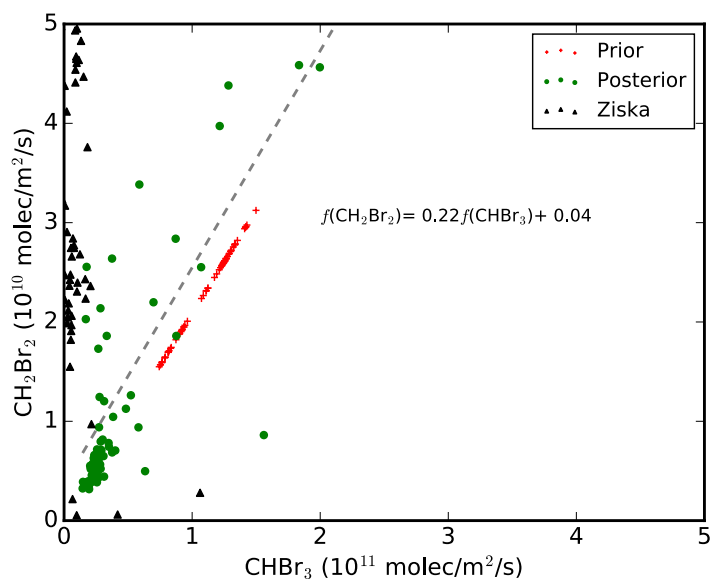


Figure 4: *A priori* and *a posteriori* (top) CHBr_3 (10^{11} molec/ m^2/s) and (bottom) CH_2Br_2 (10^{10} molec/ m^2/s) surface fluxes over the Western Pacific study region. The left panels show the *a priori* fluxes we use in our MAP inversion (Ordóñez et al., 2012); the middle panels shows an alternative bottom-up emission inventory (Ziska et al, 2013); and the right panels show our *a posteriori* flux estimates inferred from CAST and CONTRAST boundary layer data.

485



490 **Figure 5:** Scatterplot between a *priori* and a *posteriori* CHBr_3 and CH_2Br_2 fluxes described
on 2° (latitude) \times 2.5° (longitude) grid boxes over a sub-region (130° – 155°E and 0° – 12°N)
of the study region (Figure 1), where observations are most dense. Red crosses represent
values from Ordóñez et al., 2012 that we use for our *a priori*; black triangles represent values
from an alternative bottom-up inventory (Ziska et al, 2013); and green circles denote our *a*
495 *posteriori* values. A *posteriori* fluxes of CHBr_3 and CH_2Br_2 have a Pearson correlation of
0.86. The best-fit linear model for the *posteriori* fluxes is shown inset.



References

- 500 Andrews, S. J., Carpenter, L. J., Apel, E. C., Atlas, E., Donets, V., Hopkins, J. F., Hornbrook, R. S., Lewis, A. C., Lidster, R. T., Lueb, R., Minaeian, J., Navarro, M., Punjabi, S., Riemer, D., and Schauffler, S.: A comparison of very short-lived halocarbon (VSLs) and DMS aircraft measurements in the Tropical West Pacific from CAST, ATTREX and CONTRAST, Atmospheric Measurement Techniques Discussions, 2016, 1–23, doi:10.5194/amt-2016-94,
- 505 <http://www.atmos-meas-tech-discuss.net/amt-2016-94/>, 2016.
- Aschmann, J., Sinnhuber, B.-M., Atlas, E. L., and Schauffler, S. M.: Modeling the transport of very short-lived substances into the tropical upper troposphere and lower stratosphere, Atmos. Chem. Phys., 9, 9237–9247, doi:10.5194/acp-9-9237-2009, 2009.
- 510
- Ashfold, M. J., Harris, N. R. P., Manning, A. J., Robinson, A. D., Warwick, N.J., and Pyle, J. A.: Estimates of tropical bromoform emissions using an inversion method, Atmos. Chem. Phys., 14, 979–994, doi:10.5194/acp-14-979-2014, 2014.
- 515
- Butler, J. H., King, D. B., Lobert, J. M., Montzka, S. A., Yvon-Lewis, S. A., Hall, B. D., Warwick, N. J., Mondeel, D. J., Aydin, M., and Elkins, J. W.: Oceanic distributions and emissions of short-lived halocarbons, Global Biogeochem. Cy., 21, GB1023, doi:10.1029/2006GB002732, 2007.
- 520
- Butler, R., Palmer, P. I., Feng, L., Andrews, S. J., Atlas, E. L., Carpenter, L. J., Donets, V., Harris, N. R. P., Montzka, S. A., Pan, L. L., Salawitch, R. J., and Schauffler, S. M.: Quantifying the vertical transport of CHBr_3 and CH_2Br_2 over the Western Pacific, Atmos. Chem. Phys. Discuss., doi:10.5194/acp-2016-936, in review, 2016.
- 525
- Carpenter, L. J. and Liss, P. S.: On temperate sources of bromoform and other reactive organic bromine gases, J. Geophys. Res.-Atmos., 105, 20539–20547, doi:10.1029/2000JD900242, 2000.
- 530
- Carpenter, L. J., Jones, C. E., Dunk, R. M., Hornsby, K. E., and Woeltjen, J.: Air-sea fluxes of biogenic bromine from the tropical and North Atlantic Ocean, Atmos. Chem. Phys., 9, 1805–5 1816, doi:10.5194/acp-9-1805-2009, 2009.
- Carpenter, L. J., Reimann, S., Burkholder, J. B., Clerbaux, C., Hall, B.D., Hossaini, R., Laube, J. C., and Yvon-Lewis, S. A.: Update on ozone-depleting substances (ODSs) and other



535 gases of interest to the Montreal protocol, Scientific Assessment of Ozone Depletion: 2014,
2014.

Dorf, M., Butz, a., Camy-Peyret, C., Chipperfield, M. P., Kritten, L., and Pfeilsticker, K.:
Bromine in the tropical troposphere and stratosphere as derived from balloon-borne BrO
540 observations, Atmos. Chem. Phys. Discuss., 8, 12 999–13 015, doi:10.5194/acpd-8-12999-
2008, <http://www.atmos-chem-phys-discuss.net/8/12999/2008/>, 2008.

Feng, L., Palmer, P. I., Bösch, H., and Dance, S.: Estimating surface CO₂ fluxes from space-
borne CO₂ dry air mole fraction observations using an ensemble Kalman Filter, Atmos.
545 Chem. Phys., 9, 2619–2633, <https://doi.org/10.5194/acp-9-2619-2009>, 2009.

Gschwend, P. M., Macfarlane, J. K., and Newman, K. A.: Volatile halogenated organic
compounds released to seawater from temperate marine macroalgae, Science, 227, 1033–
550 1035, doi:10.1126/science.227.4690.1033, 1985.

Harris, N. R. P., Carpenter, L. J., Lee, J. D., Vaughan, G., Filus, M. T., Jones, R. L., Ouyang,
B., Pyle, J. A., Robinson, A. D., Andrews, S. J., Lewis, A.C., Minaeian, J., Vaughan, A.,
Dorsey, J. R., Gallagher, M., Le Breton, M., Newton, R., Percival, C. J., Ricketts, H. M. A.,
Bauguitte, S. J.-B., Nott, G. J., Wellpott, A., Ashfold, M. J., Flemming,; Butler, R., Palmer, P.
555 I., Kaye, P. H., Stopford, C., Chemel, C., Boesch, H., Humpage, N., Vick, A., MacKenzie, A.
R., Hyde, R., Angelov, P., Meneguz, E., Manning, A. J., Co-ordinated Airborne Studies in the
Tropics (CAST). Bull. Amer. Meteor. Soc., 98, 145–162, doi:10.1175/BAMS-D-14-00290.1,
2017.

560 Hosking, J. S., Russo, M. R., Braesicke, P., and Pyle, J. A.: Modelling deep convection and
its impacts on the tropical tropopause layer, Atmos. Chem. Phys., 10, 11175–11188,
doi:10.5194/acp-10-11175-2010, 2010.

Hossaini, R., Chipperfield, M. P., Feng, W., Breider, T. J., Atlas, E., Montzka, S. A., Miller, B.
565 R., Moore, F., and Elkins, J.: The contribution of natural and anthropogenic very short-lived
species to stratospheric bromine, Atmos. Chem. Phys., 12, 371–380, doi:10.5194/acp-12-25
371-2012, 2012.

Hossaini, R., Mantle, H., Chipperfield, M. P., Montzka, S. A., Hamer, P., Ziska, F., Quack, B.,
570 Krüger, K., Tegtmeier, S., Atlas, E., Sala, S., Engel, A., Bönisch, H., Keber, T., Oram, D.,
Mills, G., Ordóñez, C., Saiz-Lopez, A., Warwick, N., Liang, Q., Feng, W., Moore, F., Miller, B.



R., Marécal, V., Richards, N. A., D., Dorf, M., and Pfeilsticker, K.: Evaluating global emission inventories of biogenic bromocarbons, *Atmos. Chem. Phys.*, 13, 11819–11838, doi:10.5194/acp-13-11819-2013, 2013.

575

Hossaini, R., Chipperfield, M. P., Montzka, S. A., Rap, A., Dhomse, S., and Feng, W.: Efficiency of short-lived halogens at influencing climate through depletion of stratospheric ozone, *Nat. Geosci.*, 8, 186–190, doi:10.1038/ngeo2363, 2015.

580

Hossaini, R., Patra, P.K., Leeson, A. A., Krysztofiak, G., Abraham, N. L., Andrews, S. J., Archibald, A. T., Aschmann, J., Atlas, E. L., Belikov, D. A., Bönisch, H., Carpenter, L. J., Dhomse, S., Dorf, M., Engel, A., Feng, W., Fuhlbrügge, S., Griffiths, P. T., Harris, N. R. P., Hommel, R., Keber, T., Krüger, K., Lennartz, S. T., Maksyutov, S., Mantle, H., Mills, G. P., Miller, B., Montzka, S. A., Moore, F., Navarro, M. A., Oram, D. E., Pfeilsticker, K., Pyle, J.A., Quack, B., Robinson, A.D., Saikawa, E., Saiz-Lopez, A., Sala, S., Sinnhuber, B.-M., Taguchi, S., Tegtmeier, S., Lidster, R. T., Wilson, C., and Ziska, F.: A multi-model intercomparison of halogenated very short-lived substances (TransComVSLs): linking oceanic emissions and tropospheric transport for a reconciled estimate of the stratospheric source gas injection of bromine, *Atmos. Chem. Phys.*, 16, 9163–9187, doi:10.5194/acp16-9163-

590

2016, 2016a.

Hossaini, R., Chipperfield, M. P., Montzka, S. A., Leeson, A. A., Dhomse, S. S., and Pyle, J. A.: The increasing threat to stratospheric ozone from dichloromethane, *Nat. Comm.*, 8, 15962, doi: 10.1038/ncomms15962, 2016b

595

Jones, C. E., Andrews, S. J., Carpenter, L. J., Hogan, C., Hopkins, F. E., Laube, J. C., Robinson, A. D., Spain, T. G., Archer, S. D., Harris, N. R. P., Nightingale, P. D., O'Doherty, S. J., Oram, D. E., Pyle, J. A., Butler, J. H., and Hall, B. D.: Results from the first national UK inter-laboratory calibration for very short-lived halocarbons, *Atmos. Meas. Tech.*, 4, 865–874, doi:10.5194/amt-4-865-2011, 2011.

600

Law, K. S., and W. T. Sturges: Halogenated very short-lived substances, in *Scientific Assessment of Ozone Depletion: 2006*, Global Ozone Research and Monitoring Project, Rep. 50, Chap. 2, World Meteorol. Organ., Geneva, Switzerland, 2007.

605

Leedham, E. C., Hughes, C., Keng, F. S. L., Phang, S.-M., Malin, G., and Sturges, W. T.: Emission of atmospherically significant halocarbons by naturally occurring and farmed tropical macroalgae, *Biogeosciences*, 10, 3615–3633, doi:10.5194/bg-10-3615-2013, 2013.



- 610 Levine, J. G., Braesicke, P., Harris, N. R. P., Savage, N. H., and Pyle, J. A.: Pathways and timescales for troposphere-to-stratosphere transport via the tropical tropopause layer and their relevance for very short lived substances, *J. Geophys. Res.-Atmos.*, 112, D04308, doi:10.1029/2005JD006940, 2007.
- 615 Liu, Y., Shari A. Yvon-Lewis, Daniel C. O. Thornton, James H. Butler, Thomas S. Bianchi, Lisa Campbell, Lei Hu, and Smith, R.: Spatial and temporal distributions of bromoform and dibromomethane in the Atlantic Ocean and their relationship with photosynthetic biomass, *J. Geophys. Res. Oceans*, 118, 2169-9291, DOI: 10.1002/jgrc.20299, 2013.
- 620 Liang, Q., Stolarski, R. S., Kawa, S. R., Nielsen, J. E., Douglass, A. R., Rodriguez, J. M., Blake, D. R., Atlas, E. L., and Ott, L. E.: Finding the missing stratospheric Bry: a global modeling study of CHBr₃ and CH₂Br₂, *Atmos. Chem. Phys.*, 10, 2269–2286, doi:10.5194/acp10-2269-2010, 2010.
- 625 Manley, S. L., Goodwin, K., and North, W. J.: Laboratory production of bromoform, methylene bromide, and methyl iodide by macroalgae and distribution in nearshore southern California waters, *Limnol. Oceanogr.*, 37, 1652–1659, 1992.
- 630 Montzka, S. A. and Reimann, S.: Ozone-Depleting Substances (ODSs) and Related Chemicals, vol. Scientific Assessment of Ozone Depletion: 2010, Global Ozone Research and Monitoring Project – Report No. 52, chap. 1, World Meteorological Organization (WMO), Geneva, 2011.
- 635 O'Brien, L. M., Harris, N. R. P., Robinson, A. D., Gostlow, B., Warwick, N., Yang, X., and Pyle, J. A.: Bromocarbons in the tropical marine boundary layer at the Cape Verde Observatory – measurements and modelling, *Atmos. Chem. Phys.*, 9, 9083-9099, doi:10.5194/acp-9-9083-2009, 2009.
- 640 Oman, L., Douglass, D., A. R., Salawitch, R., Canty, J., T., Ziemke, P. J. R., and . Manyin : The effect of representing bromine from VLSL on the simulation and evolution of Antarctic ozone, *Geophys. Res. Lett.*, 43, 9869–9876, doi:10.1002/2016GL070471, 2016.
- Ordóñez, C., Lamarque, J.-F., Tilmes, S., Kinnison, D. E., Atlas, E. L., Blake, D. R., Sousa Santos, G., Brasseur, G., and Saiz-Lopez, A.: Bromine and iodine chemistry in a global



645 chemistry-climate model: description and evaluation of very short-lived oceanic sources,
Atmos. Chem. Phys., 12, 1423–1447, doi:10.5194/acp-12-1423-2012, 2012.

Palmer, C. J. and Reason, C. J.: Relationships of surface bromoform concentrations with
mixed layer depth and salinity in the tropical oceans, Global Biogeochem. Cy., 23, GB2014,
650 doi:10.1029/2008GB003338, 2009.

Palmer, P. I., J. J. Barnett, J. R. Eyre, and S. B. Healy, A nonlinear optimal estimation
inverse method for radio occultation measurements, J. Geophys. Res., 105, 17513-17526,
2000.

655

Pan, L. L., Atlas, E. L., Salawitch, R. J., Honomichl, S. B., Bresch, J. F., Randel, W. J., Apel,
E. C., Hornbrook, R. S., Weinheimer, A. J., Anderson, D. C., Andrews, S. J., Beaton, S. P.,
Campos, T. L., Carpenter, L. J., Chen, D., Dix, B., Donets, V., Hall, S. R., Hanisco, T. F.,
Homeyer, C. R., Huey, L. G., Jensen, J. B., Kaser, L., Kinnison, D. E., Koenig, T. K.,
660 Lamarque, J.-F., Liu, C., Luo, J., Luo, Z. J., Montzka, D. D., Nicely, J. M., Pierce, R. B.,
Riemer, D. D., Robinson, T., Romashkin, P., Saiz-Lopez, A., Schauffler, S., Shieh, O.,
Vaughan, G., Ullmann, K., Volkamer, R., Wolfe, G., Stell, M. H., and Baidar, S.: The
CONvective TRansport of Active Species in the Tropics (CONTRAST) Experiment, B. Am.
Meteorol. Soc., doi:10.1175/BAMS-D-14-00272.1, 2016.

665

Parrella, J. P., Jacob, D. J., Liang, Q., Zhang, Y., Mickley, L. J., Miller, B., Evans, M. J.,
Yang, X., Pyle, J. a., Theys, N., and Van Roozendaal, M.: Tropospheric bromine chemistry:
implications for present and pre-industrial ozone and mercury, Atmos. Chem. Phys., 12,
6723–6740, doi:10.5194/acp-12-6723-2012, [http://www.atmos-chem-](http://www.atmos-chem-phys.net/12/6723/2012/)
670 [phys.net/12/6723/2012/](http://www.atmos-chem-phys.net/12/6723/2012/), 2012.

Penkett, S. A., Engel, A., Stimpfle, R. M., Chan, K. R., Weisenstein, D. K., Ko, M. K. W., and
Salawitch, R. J.: Distribution of halon in the upper troposphere and lower stratosphere and
the 1994 total bromine budget, J. Geophys. Res.-Atmos., 103, 1513–1526,
675 doi:10.1029/97JD02466, 1998.

Pisso, I., Haynes, P. H., and Law, K. S.: Emission location dependent ozone depletion
potentials for very short-lived halogenated species, Atmos. Chem. Phys., 10, 12025–12036,
doi:10.5194/acp-10-12025-2010, 2010.

680



- Quack, B. and Suess, E.: Volatile halogenated hydrocarbons over the western Pacific between 43°S and 4° N, *J. Geophys. Res.-Atmos.*, 104, 1663–1678, doi:10.1029/98JD02730, 1999.
- 685 Quack, B. and Wallace, D. W. R.: Air-sea flux of bromoform: controls, rates, and implications, *Global Biogeochem. Cy.*, 17, 1023, doi:10.1029/2002GB001890, 2003.
- Quack, B., Atlas, E., Petrick, G., and Wallace, D. W. R.: Bromoform and dibromomethane above the Mauritanian upwelling: Atmospheric distributions and oceanic emissions, *J. Geophys. Res.- Atmos.*, 112, D09312, doi:10.1029/2006JD007614, 2007.
- 690 Quack, B., Atlas, E., Petrick, G., and Wallace, D. W. R.: Bromoform and dibromomethane above the Mauritanian upwelling: Atmospheric distributions and oceanic emissions, *J. Geophys. Res.- Atmos.*, 112, D09312, doi:10.1029/2006JD007614, 2007.
- Read, K. A., Mahajan, A. S., Carpenter, L. J., Evans, M. J., Faria, B. V. E., Heard, D. E., Hopkins, J. R., Lee, J. D., Moller, S. J., Lewis, A. C., Mendes, L., McQuaid, J. B., Oetjen, H., Saiz, Lopez, A., Pilling, M. J., and Plane, J. M. C.: Extensive halogen-mediated ozone destruction over the tropical Atlantic Ocean, *Nature*, 453, 1232–1235, doi:10.1038/nature07035, 2008.
- 695 Read, K. A., Mahajan, A. S., Carpenter, L. J., Evans, M. J., Faria, B. V. E., Heard, D. E., Hopkins, J. R., Lee, J. D., Moller, S. J., Lewis, A. C., Mendes, L., McQuaid, J. B., Oetjen, H., Saiz, Lopez, A., Pilling, M. J., and Plane, J. M. C.: Extensive halogen-mediated ozone destruction over the tropical Atlantic Ocean, *Nature*, 453, 1232–1235, doi:10.1038/nature07035, 2008.
- Russo, M. R., Ashfold, M. J., Harris, N. R. P., and Pyle, J. A.: On the emissions and transport of bromoform: sensitivity to model resolution and emission location, *Atmos. Chem. Phys.*, 15, 14031–14040, <https://doi.org/10.5194/acp-15-14031-2015>, 2015.
- 700 Russo, M. R., Ashfold, M. J., Harris, N. R. P., and Pyle, J. A.: On the emissions and transport of bromoform: sensitivity to model resolution and emission location, *Atmos. Chem. Phys.*, 15, 14031–14040, <https://doi.org/10.5194/acp-15-14031-2015>, 2015.
- Stemmler, R., Hill, K. M., and Folini, D.: Low European methyl chloroform emissions inferred from long-term atmospheric measurements, *Nature*, 433, 506–508, doi:10.1038/nature03220, 2005.
- 705 Stemmler, R., Hill, K. M., and Folini, D.: Low European methyl chloroform emissions inferred from long-term atmospheric measurements, *Nature*, 433, 506–508, doi:10.1038/nature03220, 2005.
- Salawitch, R. J., Canty, T., Kurosu, T., Chance, K., Liang, Q., da Silva, A., Pawson, S., Nielsen, J. E., Rodriguez, J. M., Bhartia, P. K., Liu, X., Huey, L. G., Liao, J., Stickel, R. E., Tanner, D. J., Dibb, J. E., Simpson, W. R., Donohoue, D., Weinheimer, A., Flocke, F., Knapp, D., Montzka, D., Neuman, J. A., Nowak, J. B., Ryerson, T. B., Oltmans, S., Blake, D. R., Atlas, E. L., Kinnison, D. E., Tilmes, S., Pan, L. L., Hendrick, F., Van Roozendaal, M., Kreher, K., Johnston, P. V., Gao, R. S., Johnson, B., Bui, T. P., Chen, G., Pierce, R. B., Crawford, J. H., and Jacob, D. J.: A new interpretation of total column BrO during Arctic spring, *Geophysical Research Letters*, 37, doi:10.1029/2010GL043798, <http://dx.doi.org/10.1029/2010GL043798>, I21805, 2010.
- 710 Salawitch, R. J., Canty, T., Kurosu, T., Chance, K., Liang, Q., da Silva, A., Pawson, S., Nielsen, J. E., Rodriguez, J. M., Bhartia, P. K., Liu, X., Huey, L. G., Liao, J., Stickel, R. E., Tanner, D. J., Dibb, J. E., Simpson, W. R., Donohoue, D., Weinheimer, A., Flocke, F., Knapp, D., Montzka, D., Neuman, J. A., Nowak, J. B., Ryerson, T. B., Oltmans, S., Blake, D. R., Atlas, E. L., Kinnison, D. E., Tilmes, S., Pan, L. L., Hendrick, F., Van Roozendaal, M., Kreher, K., Johnston, P. V., Gao, R. S., Johnson, B., Bui, T. P., Chen, G., Pierce, R. B., Crawford, J. H., and Jacob, D. J.: A new interpretation of total column BrO during Arctic spring, *Geophysical Research Letters*, 37, doi:10.1029/2010GL043798, <http://dx.doi.org/10.1029/2010GL043798>, I21805, 2010.

715



- Stemmler, I., Hense, I., and Quack, B.: Marine sources of bromoform in the global open ocean – global patterns and emissions, *Biogeosciences*, 12, 1967-1981, doi:10.5194/bg-12-1967-2015, 2015.
- 720 Sturges, W.T., Cota, G.F., and Buckley, P.T.: Bromoform emission from Arcticic ealgae, *Nature*, 358, 660–662, doi:10.1038/358660a0, 1992.
- Tokarczyk, R. and Moore, R. M.: Production of volatile organohalogens by phytoplankton cultures, *Geophys. Res. Lett.*, 21, 285–288, doi:10.1029/94GL00009, 1994.
- 725 Warwick, N. J., Pyle, J. A., Carver, G. D., Yang, X., Savage, N. H., O'Connor, F. M., and Cox, R. A.: Global modeling of biogenic bromocarbons, *J. Geophys. Res.-Atmos.*, 111, D24305, doi:10.1029/2006JD007264, 2006.
- 730 Yang, X., Cox, R. A., Warwick, N. J., Pyle, J. A., Carver, G. D., O'Connor, F. M., and Savage, N. H.: Tropospheric bromine chemistry and its impacts on ozone: a model study, *J. Geophys. Res.-Atmos.*, 110, D23311, doi:10.1029/2005JD006244, 2005.
- Ziska, F., Quack, B., Abrahamsson, K., Archer, S. D., Atlas, E., Bell, T., Butler, J. H.,
735 Carpenter, L. J., Jones, C. E., Harris, N. R. P., Hepach, H., Heumann, K. G., Hughes, C., Kuss, J., Krüger, K., Liss, P., Moore, R. M., Orlikowska, A., Raimund, S., Reeves, C. E., Reifenhäuser, W., Robinson, A. D., Schall, C., Tanhua, T., Tegtmeier, S., Turner, S., Wang, L., Wallace, D., Williams, J., Yamamoto, H., Yvon-Lewis, S., and Yokouchi, Y.: Global sea-to-air flux climatology for bromoform, dibromomethane and methyl iodide, *Atmos. Chem. Phys.*, 13, 8915-8934, <https://doi.org/10.5194/acp-13-8915-2013>, 2013.
- 740